Tellus (1999), 51B, 766–788
Printed in UK – all rights reserved

TELLUS
ISSN 0280–6495

Effects of lightning and convection on changes in tropospheric ozone due to NO_x emissions from aircraft

By TERJE K. BERNTSEN* and IVAR S. A. ISAKSEN, *Department of Geophysics, University of Oslo, PO Box 1022, Blindern, 0315 Oslo, Norway; Center for International Climate and Environmental Research — Oslo (CICERO), PO Box 1129, Blindern, 0317 Oslo, Norway*

(Manuscript received 19 January 1998; in final form 25 March 1999)

ABSTRACT

A global 3-dimensional chemical tracer model (CTM) has been used to calculate the impact on tropospheric ozone caused by NO_x emissions from today's fleet of subsonic aircraft (0.52 Tg(N)/yr). Uncertainties in the magnitude and distribution in the ozone perturbation due to uncertainties in lightning and deep convection as sources of upper tropospheric NO_x have been studied. Three sets of two CTM experiments have been performed, with and without emissions from aircraft. A reference set with normal convection and 12 Tg(N)/yr from lightning, a set with reduced lightning source (5 Tg(N)/yr), and one set with reduced convective activity (67% lower mass fluxes of air). A zonally homogeneous increase in upper tropospheric ozone north of 40°N, reaching a maximum of 5–6 ppbv during May was found in the reference case. The largest effect of lower NO_x emissions from lightning was a 50–70% higher enhancement of ozone due to aircraft at northern mid- and high-latitudes during summer. This was caused by lower background concentrations of NO_x and therefore more efficient ozone production. Reduced convective mixing lead to a 40% increased enhancement in aircraft induced ozone at northern mid-latitudes and 150% enhancement in the tropics. In this case background NO_x levels were higher in the upper troposphere, giving a decreased ozone production efficiency of NO_x from aircraft. This was however, more than compensated for by a decreased downward mixing of ozone produced by emissions from aircraft.

1. Introduction

Emissions of NO_x from subsonic aircraft have the potential to increase the natural level of ozone in the upper troposphere and lower stratosphere significantly. However, there are significant discrepancies in the influence of subsonic aircraft estimated by global photochemical transport models (Brasseur et al., 1998). The non-linear nature of the ozone production as a function of the background NO_x levels, and the substantial uncertainties in the NO_x budgets in this region of the atmosphere, could be a major factor contributing to this. In this study we a global 3-dimensional chemical tracer model (Berntsen and Isaksen, 1997) to investigate how uncertainties in two of the major processes affecting the upper tropospheric NO_x levels, namely lightning and convection influence the estimated impact of aircraft emissions.

Changes in ozone in the upper troposphere will have significantly larger effects on radiative forcing (RF) of climate than changes in other altitude regions of the atmosphere (Wang and Sze, 1980; Lacis et al., 1990; IPCC, 1992). Model studies of the impact of increased emissions of ozone precursors since pre-industrial times indicate that the increase in tropospheric ozone has caused a global averaged RF of 0.2–0.6 W/m^2 (IPCC-95). This is about 20% of the increase in forcing caused by

* Corresponding author.

the increase in the concentrations of well-mixed greenhouse gases (Hauglustaine et al., 1994; Lelieveld and Van Dorland 1995; Forster et al., 1996; Berntsen et al., 1997).

The sources of ozone in the troposphere are in situ chemical reactions involving nitrogen oxides ($NO_x = NO + NO_2$), methane (CH_4), carbon monoxide (CO), non-methane hydrocarbons (NMHCs) and sunlight (Crutzen, 1973), and intrusion of ozone rich air from the stratosphere. The efficiency of the ozone formation per NO_x molecule oxidised is a highly non-linear function of the ambient NO_x levels (Isaksen et al., 1978; Lin at al., 1988). Emissions of NO_x from aircraft in the upper troposphere take place in an environment with generally lower levels of NO_x than in the continental planetary boundary layer (PBL). Due to the combination of chemical and radiative effects NO_x from aircraft is expected to have a much higher impact on climate than similar emissions from surface sources (WMO, 1995; Fuglestvedt et al., 1996).

NO_x emissions generally increase OH concentration and thereby decrease methane concentrations. The radiative forcing of the lower methane concentrations tends to be of the opposite sign and of similar magnitude as the impact on ozone for *surface* sources of NO_x. Previous studies with 2-D models have indicated that for NO_x from aircraft the effect on methane is smaller due to lower humidity and temperatures in the upper troposphere (Fuglestvedt et al., 1996). However, more recent studies (IPCC, 1999) with 3-D models find that the global mean radiative forcing due to methane changes are of similar magnitude as for the changes in ozone. The nature of the forcing due to methane changes is very different since methane perturbations are more homogeneous spatially, and occurs on a much longer time-scale than ozone. The impact on climate through the combined effect of ozone and methane will probably not be cancelled out.

The total source of NO_x from aircraft for the present fleet of subsonic aircraft has been estimated to be of about 0.5 Tg(N)/yr, with a projected increase in fuel use of 3–5%/yr until 2015 (Jenkins, 1996). Other sources of NO_x in the upper troposphere include lightning (2–20 Tg(N)/yr), transport from the PBL by deep convection, input from the stratosphere (<1 Tg(N)/yr) and recycling of NO_y species (HNO_3, HO_2NO_2, and PAN) through thermal decomposition, photolysis and possibly heterogeneous processes (Hauglustaine et al., 1996). Several model studies have addressed the question of the impact of the emissions from aircraft on upper tropospheric NO_x, NO_y, and ozone (Brasseur et al., 1996; Schumann, 1997a; Schumann, 1997b; Wauben et al., 1997; Stevenson et al., 1997; Dameris et al., 1998). However, due to the non-linear dependence of the ozone formation, uncertainties in the other sources of upper tropospheric NO_x could have a significant influence on the estimated changes in ozone distribution.

In this work, we use the University of Oslo 3-D global chemical tracer model (CTM) (Berntsen and Isaksen, 1997; Jaffe et al., 1997; Berntsen et al., 1997) to study how the uncertainties in deep convection and lightning sources of upper tropospheric NO_x influence the estimated increase in upper tropospheric ozone from aircraft. The CTM is the same as was used for the "Special Report on Aviation and the Global Atmosphere", (IPCC, 1999). The results from our calculations (with other emissions from aircraft, and a total NO_x source from lightning of 5 Tg(N)/yr) were found to represent a central estimate of the CTM results, and were therefore chosen for calculations of radiative forcing and changes in UV. Estimates of emissions of NO_x from lightning discharges are based on a number of parameters that are subject to uncertainties. This includes total number of lightning flashes, energy dissipation per flash, NO production mechanism and efficiency, altitude distribution, relative efficiency of cloud-to-ground (CG) strokes and cloud-to-cloud strokes, etc. (Gallardo and Cooray, 1996; Price et al., 1997a). In this study we focus only on the effects of the total NO_x emissions from lightning. Therefore we have applied the same relative horizontal, vertical and temporal distribution of the lightning source of NO_x in all the model experiments.

The impact of NO_x emissions from aircraft on upper tropospheric ozone in a base case with 12 Tg(N)/yr from lightning and with standard convective mixing (from the NASA/GISS GCM, see Prather et al., 1987 for details) have been compared with the corresponding impact of aircraft in two perturbation cases. In case LL, the lightning source of NO_x is reduced to 5 Tg(N)/yr, while in case LC the convective activity in the model is reduced by 67%. The rationale for choos-

ing these two experiments (cf. Subsection 2.2) is based on recent studies of lightning emissions (Price et al., 1997a, 1997b) and convective mixing in CTMs (Jacob et al., 1997). Uncertainties caused by limitations in our understanding of stratosphere/troposphere exchange processes is not addressed in this paper due to limitations in the vertical resolution of the model in the tropopause region.

2. Model description

The model has been discussed in detail elsewhere (Prather et al., 1987; Berntsen and Isaksen, 1997; Berntsen et al., 1997), hence only a short description will be given here.

The CTM has a resolution of 8° by 10° (latitude versus longitude) and 9 vertical layers below 10 hPa. The vertical resolution in the vicinity of the tropopause is about 3 km at mid- and high-latitudes, and about 4.5 km in the tropics. The transport formulation includes 3-dimensional advection, calculated by the very accurate "second order moments" method of Prather (1986), as well as rapid vertical mixing by convective transport (Prather et al., 1987). The strength of the deep convective transport is quite uncertain. Jacob et al. (1997) have compared vertical mixing of radon (^{222}Rn) in various CTMs, including the GISS/H/I model which has a very similar transport parameterisation as our CTM. They conclude that the simulated deep convection in the troposphere is within the constraints offered by seasonal averages of ^{222}Rn concentrations at different altitudes.

A comprehensive photochemical scheme with 55 chemical components and 120 gas-phase reactions has been incorporated to simulate the photochemistry of the troposphere. For this work the chemistry scheme has been extended to include degradation of propane, which gives acetone which has been found to be a major constituent, and a potentially important source of HO_x, in the upper troposphere (Singh et al., 1995; Arnold et al., 1997; McKeen et al., 1997). So far no direct emissions of acetone are included, thereby giving too low concentrations of acetone in the model. Within the troposphere, the chemistry with a full diurnal cycle is calculated with a quasi steady-state approximation method (QSSA), with iterations for the short-lived species (Hesstvedt et al., 1978). In the stratosphere, concentrations of ozone, NO_x and HNO_3 are fixed according to the observed distribution of these species. The circulation within the whole model domain up to 10 hPa then generates an internally consistent cross-tropopause flux. The photolysis rates have been calculated with the two-stream algorithm of Kylling et al. (1995). The model uses pre-calculated meteorological input data with 8-h time resolution from a one-year climate simulation with the NASA/GISS GCM. The continuity equation is solved by an operator splitting procedure with a 1-h time-step for the transport, and 30 min for the chemistry.

In this study, chemistry calculations have been done up to about 18.5 km altitude ($\sigma = 0.061$) in the tropics (equator-ward of 32°), and up to about 13.7 km ($\sigma = 0.144$) at higher latitudes. Above these altitudes the concentrations of O_3, NO_x and HNO_3 were prescribed as described in Berntsen et al. (1997).

A relevant question to ask is whether it is appropriate to use a coarse resolution 3-D model like this to study effects on ozone due to trends in upper atmospheric sources of NO_x like aircraft given the non-linear dependence of the ozone production on the background NO_x concentrations. However, Flatøy and Hov (1996) used a mesoscale CTM (150 km resolution) to address the impact of NO_x from aircraft, and conclude that the non-linear effects of the background NO_x levels did not alter the influence of NO_x from aircraft significantly.

2.1. Convection

Rapid vertical transport within deep convective cells can transport air originating in the PBL to the upper troposphere within less than an hour. Short-lived species like NO_x can therefore be transported to the upper troposphere in significant amounts. Strand and Hov (1996) estimate in a 2-D zonally averaged model that rapid mixing within convective cells and frontal zones contribute about 0.7 Tg(N)/yr of NO_x from the PBL to the free troposphere for the month of July. Köhler et al. (1997) find in a 3-D CTM a contribution from surface sources to the upper tropospheric NO_x burden at northern mid-latitudes of about 10 and 25% for January and July, respectively. An important aspect of convective transport of

NO_x from the surface is the positive correlation between regions of intense deep convection and elevated concentrations of NO_x in the PBL (i.e., continental regions) at least at northern mid-latitudes where most of the emissions from aircraft take place. Due to these factors and the non-linear ozone chemistry, we believe it is important to apply a 3-D CTM in this kind of study.

The parameterisation of vertical mixing due to convection in this CTM is described in Prather et al. (1987). It includes rapid updrafts in the thermals and slower subsidence of the surrounding cloud free air. The vertical transport in the updrafts is the net transport within the convective cell, i.e., updraft–downdraft. The effect of downdrafts is not represented explicitly. In this CTM the net effect of convective mixing is to deposit about 120 Gg(N)/month to the upper troposphere of the northern hemisphere (390–150 hPa) for the month of July. Correspondingly, lightning (case *R*, 12 Tg(N)/yr), aircraft and stratospheric influx are found to contribute about 390, 42, and 153 Gg(N)/month respectively.

A major source of the discrepancies between earlier model estimates of the impact of aircraft emissions is differences in the terminal height of upward transport in convective cells. In some of the models the emissions from aircraft probably occur at the same altitude as the convective cloud tops (i.e., in the same vertical model layer), while in other models the two sources are normally separated. Due to the non-linearity of the chemistry the impact will be largest in the latter case. To examine how this works in this CTM, we have calculated the monthly mean deep convective mass flux from below into each vertical layer. Fig. 1 shows a comparison of the zonal mean distribution of the convective mass flux for July and the corresponding distribution of aircraft emissions. The emissions from aircraft have a maximum in model layer 7 ($\approx$ 10.3–13.7 km altitude) at 45°N, decreasing by about 75% to the model layer below ($\approx$ 7.4–10.3 km altitude). At northern mid-latitudes during summer, the maximum convective flux is deposited in layer 6. However, a significant amount (35–40% of the value in layer 6) is deposited at the altitude of maximum aircraft emissions as well. In the tropics the convection and the aircraft emissions have the largest contribution at the same altitudes. The maximum in convective flux to the middle troposphere (4–6 km) found in the southern hemisphere, is associated with frontal activity in extra tropical cyclones. A similar maximum is found in the northern hemisphere during winter.

It is difficult to compare the distribution of convective mass fluxes given in Fig. 1 with observations. Still, a comparison with the frequency

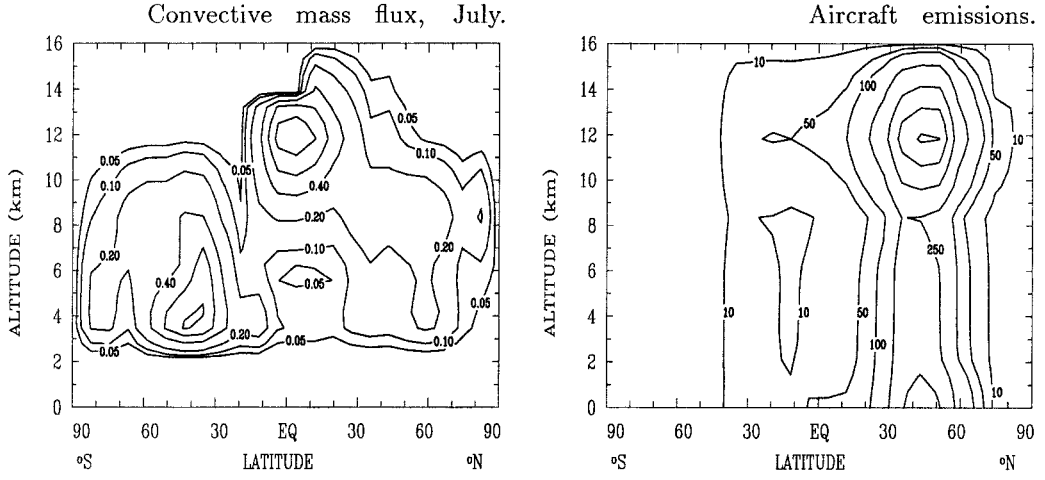

Fig. 1. Left: monthly mean zonal averaged deep convective mass flux (of air) from below to each model layer. Values are normalised, giving the gridcell with the highest flux a value of 1.0. Isolines at 0.01, 0.05, 0.1, 0.2, 0.4, 0.6, 0.8 and 1.0. Right: zonal mean distribution of aircraft emissions of NO. Isolines at 10, 50, 100, 250, 500, 750 and 1000 molecules $cm^{-3}\,s^{-1}$.

distribution of cloud top pressures from ISCCP (Rossow and Schiffer, 1991) shows that the ratio between the observed frequency of cloud top heights reaching 310 and 180 hPa respectively in July is very similar to the ratio between the convective mass fluxes to layer 6 and 7 in the CTM. This indicates that the altitude distribution of the vertical mixing by deep convection in the CTM is qualitatively correct. The amount of transport of air from the PBL aloft can of course not be inferred from the ISCCP data. Thus, the comparison above does not provide a validation of the vertical mixing by deep convective clouds in the CTM.

2.2. Experimental set-up

A total of 6, 16-month model experiments have been performed for this study. Two experiments for reference case with and without emissions from aircraft (called case R_A and R_0 respectively), two experiments with a decreased lightning source (5 Tg(N)/yr instead of 12 Tg(N)/yr as in the reference case) (cases LL_A and LL_0), and two experiments with reduced convection (cases LC_A and LC_0). In the LC experiments the number of convective events (i.e., the convective mass flux) was reduced by 67%. The rationale for choosing 5 and 12 Tg(N)/yr from lightning was that 5 Tg(N)/yr represents the most commonly used figure in previous studies, while 12 Tg(N)/yr is the result obtained from the recent study of Price et al. (1997a, 1997b). The chosen values are well within the range of 2–20 Tg(N)/yr given by IPCC (1992), and with our current understanding of the lightning source it is not possible to determine which of the two lightning sources (5 or 12 Tg(N)/yr) is most likely to be correct. To study the uncertainty caused by convective transport, we reduce the activity by 67% based on results obtained by Jacob et al. (1997). In a comparison of global atmospheric transport in 7 CTMs they found that the simulated concentration of ^{222}Rn in the upper troposphere varied by approximately this amount between the models both at northern mid-latitudes and in the tropics. In the tropics the GISS/H/I model which has a transport very similar to our CTM gave the highest concentrations, while at northern mid-latitudes the GISS/H/I model gave results about the same as the mean of the 7 CTMs.

Table 1. *Global annual emission rates applied in the model*

Species	Source	Annual emission rate
NO_x (Tg(N)/yr)	fossil fuels[a)]	21.0
	biomass burning[b)]	4.4
	soils[a)]	5.5
	lightning[c)]	12.2
	aircraft[d)]	0.52
	total	46.4
CO (Tg/yr)	anthropogenic[b)]	893
	biomass burning[b]	714
	soils[b)]	387
	oceans[b)]	378
	total	2362
isoprene[a)] (Tg/yr)	natural	570
other NMHCs[e)]	natural	64.8
	anthropogenic	114

[a)] From the GEIA inventory (http://blueskies.sprl.umich.edu/geia).
[b)] From Müller (1992) and Müller and Brasseur (1995).
[c)] From Price et al. (1997a).
[d)] From the ANCAT/DLR-2 database (Nüsser and Schmitt, 1996).
[e)] See Berntsen and Isaksen (1997) and references therein.

3. Emissions

3.1. Surface and aircraft emissions

The available emission inventories from the IGAC/GEIA database (for 1985 conditions) have been used in this work, and have been supplemented by other well-documented sources as given in Table 1.

Of particular importance for this study is the emission inventories for aircraft and lightning. The aircraft emissions are taken from the ANCAT/DLR-2 database (Nüsser and Schmitt, 1996), and include seasonal estimates of NO_x emissions from civil and military air traffic (Fig. 1). The total amount of NO_x emitted above the upper boundary for the chemistry calculations in the model (cf. Section 2.1) is only about 0.15%.

3.2. Lightning

3.2.1. Total emissions. Emissions of NO_x from lightning have been estimated in a number of studies, and the estimated total global source varies between 1 Tg(N)/yr (Levine et al., 1981)

and 100 Tg(N)/yr (Franzbleu and Popp, 1989). Recent estimates by WMO (WMO, 1995) and Lee et al. (1997) give a range of 2–20 Tg(N)/yr, with 5–7 Tg(N)/yr as most likely. In previous CTM studies, a lightning source of 3–8 Tg(N)/yr is applied (Dentener and Crutzen, 1993; Müller and Brasseur, 1995; Lelieveld and Van Dorland, 1995; Roelofs and Lelieveld, 1995; Strand and Hov, 1996; Wauben et al., 1997; Berntsen et al., 1997). Recently, Price et al. (1997a) have re-evaluated the NO_x source from lightning and arrived at a significantly higher global annual emission rate of 12.2 Tg(N)/yr. Price et al. (1997b) arrive at a similar high estimate applying an independent method, using the global atmospheric circuit to put a constraint on the global cloud to ground lightning activity.

Lightning emissions of NO_x for this study have been included in the CTM by starting out with the monthly averaged source given on a 2.5° by 2.5° grid from Price et al. (1997a) and the input data on deep convection from the GISS GCM (Hansen et al., 1983). Emission of NO_x from lightning takes place in connection with rapid vertical mixing in deep convective cells. Based on the GCM data and a parameterisation of lightning activity as a function of cloud top height for continental and marine clouds respectively (Price and Rind, 1993) we calculate the longitudinal and temporal distribution of lightning. We then use this to distribute the zonally averaged emissions from Price et al. (1997a) as a function of longitude and time (8-h resolution) according to the calculated lightning activity in each grid column. The details of the methods are given in Section 7. This procedure also assures that the lightning emissions are inserted into columns where strong vertical mixing by deep convection is occurring at the same time.

3.2.2. Vertical distribution. The rapid vertical mixing of NO_x from lightning in thunderstorms has two consequences with respect to the impact of the emissions. First, the NO_x from the lightning is redistributed vertically. Downdrafts within the storm might deposit a fair amount of NO_x close to the ground, while updrafts transport the NO_x into the top of the cloud, where it is detrained into the surrounding air. Also, the higher energy per stroke in CG strokes than in CC strokes (Price et al. 1997a), and the dependence of the NO_x production efficiency (molecules of NO_x per unit of energy) on the ambient air pressure (Goldenbaum and Dickerson, 1993), both favour NO_x production in the lower troposphere (below 5 km). Therefore, it is reason to believe that the NO_x produced by lightning gives a C-shaped profile of the mixing ratio of NO_x, even if the most efficient NO_x-producing CG flashes occur within the lower part of the cloud. Secondly, the vertical mixing brings air from the PBL, which can be enriched in NO_x and other ozone precursors from surface sources, into the free troposphere. Due to the non-linear ozone chemistry the strong correlation between strong vertical mixing and lightning can change the chemical impact of the emissions significantly (Flatøy and Hov, 1997).

The data given in Price et al. (1997a) only give the vertically integrated distribution of the sources. In this study a constant altitude emission profile of the NO_x (in pptv/time) within each thunderstorm (i.e., each deep convective event from the NASA/GISS GCM data) has been assumed (Gallardo and Cooray, 1996). This is equivalent to the assumption that the production rate on a mass per volume basis decreases proportionally with pressure. This is different than the parameterisation applied by Flatøy and Hov (1997) which distributes the emissions vertically on a mass basis according to fractional cloud cover at each vertical model layer.

As discussed above, the lightning emissions in the CTM take place in connection with deep convective events (8-h average in the meteorological input data). Thus the convective mixing in the CTM will act to redistribute the NO_x from lightning. As the current parameterisation of convective mixing in the CTM does not include downdrafts, one could expect that the amount of NO_x emitted into the upper troposphere could be overestimated. However, in the real atmosphere the NO_x is emitted directly into the region of strong vertical mixing while in the model the implicit assumption is that it is equally distributed over the whole model layer. This would tend to underestimate the fraction of the NO_x reaching the upper troposphere. To what extent these two factors balance each other and how they affect the upper tropospheric NO_x budget is difficult to determine with our current CTM.

The vertical redistribution and the extended lifetime of NO_x at higher altitudes give a maximum

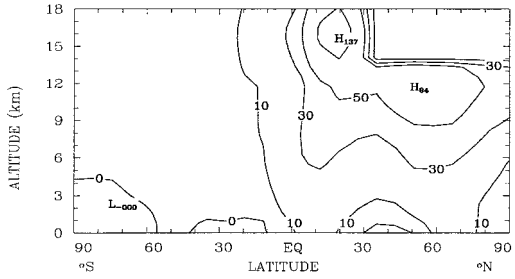

Fig. 2. Increase in zonally averaged NO_x concentrations (pptv) in July when lightning sources are included. Isolines at 0, 10, 30, 50, 100, and 150 pptv.

in the contribution of NO_x from lightning in the upper troposphere (Fig. 2). In July the contribution is strongest in the northern hemisphere over the continents. At mid-latitudes lightning contributes about 100–150 pptv over the continents, and 50–70 pptv over the oceans. The relative contribution of NO_x from lightning is largest (80%) in the middle troposphere (6–7 km altitude) in the tropics mainly due to the very low contribution from other sources in this region.

4. Results and discussion

4.1. The reference case

4.1.1. NO_x distribution in the upper troposphere. Due to the large latitudinal and longitudinal differences in the source strength of the NO_x emissions there is very significant gradients (2–3 orders of magnitude) in the NO_x concentrations in the PBL between northern mid-latitude industrialised regions and marine background regions. In the upper troposphere, the chemical lifetime of NO_x is longer, and longitudinal mixing is faster. Nevertheless, the CTM calculates significant gradients in the upper tropospheric NO_x distribution as well (Fig. 3). At northern mid-latitudes the calculated concentrations of NO_x are in reasonable agreement with observations. Fig. 4 shows a comparison between observed (Emmons et al., 1997; Schlager et al., 1997) and calculated NO concentrations (midday) in the region of the atmosphere most influenced by emissions from aircraft (northern mid- and high-latitudes) for case R_a. The model results are generally somewhat lower than the observed values, but except for two data-points, the model results are within the one standard deviation range of the measurements.

The agreement between calculated and the limited observational data set of NO_x in the upper troposphere at northern mid-latitudes is generally quite good, and better than earlier experiments with this CTM (Jaffe et al. (1997), using 5 Tg(N)/yr from lightning). This could be an indication that 12 Tg(N)/yr of NO_x from lightning is more correct. However, other factors like a different vertical distribution of lightning sources (Gallardo and Cooray, 1996), or some unknown chemistry which can recycle HNO_3 to NO_x (Chatfield, 1994; Hauglustaine et al., 1996; Jacob et al., 1996), can give the same effect on NO_x in the upper troposphere.

At lower latitudes, measurements during the

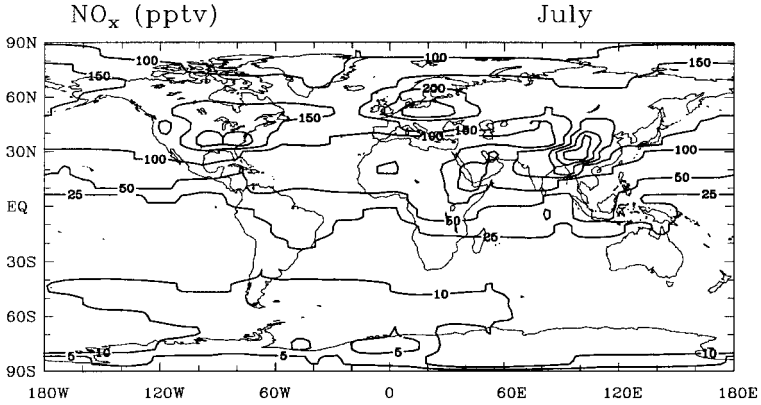

Fig. 3. Calculated monthly mean distribution of NO_x in case R_0 at approximately 12 km altitude during July. Emissions from aircraft not included. Isolines at 5, 10, 25, 50, 100, 150, 200, 250 and 300 pptv.

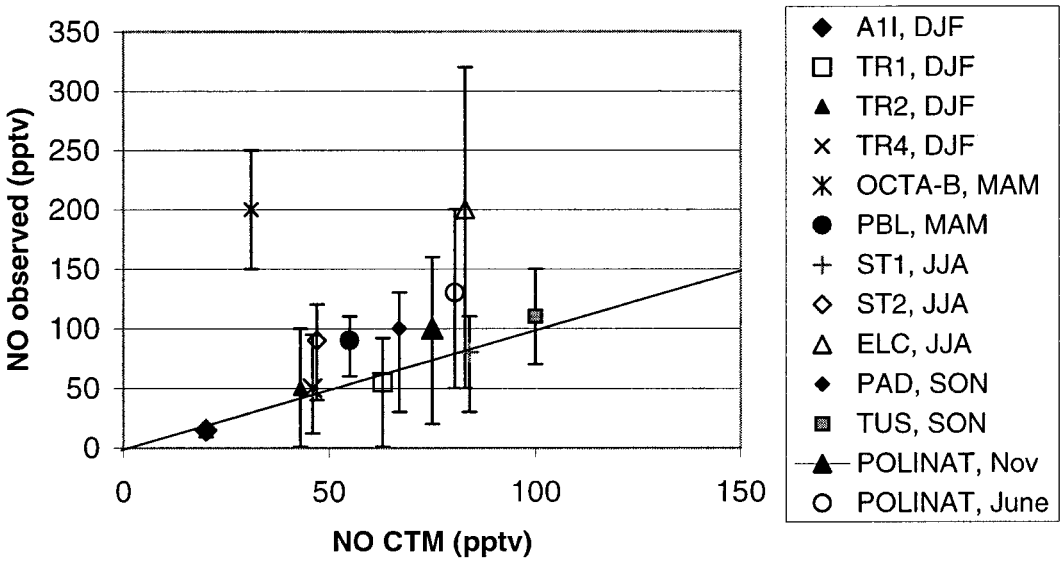

Fig. 4. Comparison of calculated and observed midday NO concentrations in the upper troposphere at northern mid-latitudes. Observations (with acronyms) adopted from Emmons et al. (1997) and Schlager et al. (1997).

TRACE A experiment presented by Jacob et al. (1996) indicate NO_x-concentrations of the order 50–500 pptv at 9–10 km altitude over Africa, South Atlantic and South America during the biomass burning season in September/October. Using a filtering technique ($CO < 80$ ppbv) to identify cases not influenced directly by biomass burning TRACE A, Singh et al. (1996b) found NO concentrations of 50–100 pptv. Over the tropical Western Pacific (0–20°N) Singh et al. (1996a) measured 25–50 pptv of NO_x in the upper troposphere. At lower latitudes the model seems to underestimate the NO_x concentrations significantly (as many other models do, Jacob et al., (1996)) even with a lightning source of 12 Tg(N)/yr. This supports the conclusion found in other studies, that there might be some unknown chemistry transforming HNO_3 to NO_x.

4.1.2. Sources of upper tropospheric NO_x. The change in the total amount of NO_x in any compartment of the free troposphere, over the course of a month, is small compared to the source and sink terms in the NO_x budget due to the short chemical lifetime. The contribution to the upper tropospheric NO_x budget from the main source processes is given in Table 2. The northern hemisphere has been divided into 7 regions. The Arctic is everywhere north of 56°N, the region between 32 and 56°N is divided into 5 regions; Pacific (157.5°E–122.5°W), North America (122.5–62.5°W), North Atlantic (62.5–12.5°W), Europe (12.5°W–47.5°E), and Asia (47.5–157.5°E). The tropics (northern and southern) are defined as the regions between the equator and 32°.

Due to the different nature of the terms in Table 2, the results must be interpreted with care. The "Convection" term is the net effect of updrafts and subsidence. Therefore, in a situation where the combination of high surface sources and convection gives a C-shaped profile of NO_x with altitude (i.e., over the continents), the net effect of convection could be close to zero. The magnitude of the convection term is also dependent on how convection and lightning emissions are linked. With a dynamical lightning source, as in this model (cf. Subsection 3.2.2), the lightning emissions occur only when there is deep moist convection in the column. The lightning emissions at lower altitudes are then transported aloft by the updrafts, leading to higher values for the convection term. In models using a climatological averaged lightning source the convection term is likely to be smaller and probably negative over large regions. Another factor which influence the convection term is that higher contributions from

Table 2. *Upper tropospheric NO_x sources (390–150 hPa) for July*

. Region	Lightning[b)]	Convection	Aircraft	Stratospheric flux[c)]
Arctic	37.2 (0.33)	1.9 (0.016)	2.20 (0.075)	7.8 (0.10)
Pacific	2.65 (0.06)	−0.56 (−0.004)	1.09 (0.095)	0.91 (0.030)
N. America	37.3 (1.00)	36.3 (0.92)	8.65 (0.86)	10.1 (0.40)
N. Atlantic	3.08 (0.12)	−0.17 (−0.006)	2.19 (0.30)	−1.4 (−0.08)
Europe	19.8 (0.62)	33.9 (1.00)	8.63 (1.00)	21.8 (1.00)
Asia	42.9 (0.80)	21.3 (0.38)	9.16 (0.64)	23.4 (0.64)
NH Tropics[a)]	243 (0.72)	52.3 (0.15)	10.4 (0.11)	−1.0 (0.004)
SH Tropics[a)]	33.2 (1.00)	29.2 (1.00)	1.81 (1.00)	6.9 (0.08)
rest SH	0.39 (0.01)	1.15 (0.04)	0.38 (0.21)	84.3 (1.00)

Values in Gg(N)/month. Numbers in ( ) are normalised flux (per area) for each source. Region with maximum flux is set equal to 1.0 in each hemisphere.
[a)] 390–70 hPa, due to the higher tropopause height at low latitudes.
[b)] 12 Tg(N)/yr from lightning.
[c)] Net downward flux of NO_x at 150 hPa (mid-latitudes), and 70 hPa in the tropics.

other sources of NO_x in the upper troposphere decrease the net contribution from convection, as the loss through subsidence increases.

Except for Europe, lightning is the largest source of upper tropospheric NO_x, in all regions. When the source terms are normalised with respect to the area of each region, the contribution from aircraft, convection and stratospheric flux is strongest over the continental mid-latitude regions. An interesting feature is that in July the contribution from lightning at high latitudes is much higher than convection, stratospheric flux, and aircraft, reaching about 50% of the value obtained for the tropical/sub-tropical region.

A major part of the NO_x transported or emitted to the upper troposphere is converted through chemical processes to longer lived NO_y species (HNO_3, PAN, HO_2NO_2, and N_2O_5) which are lost by downward transport and wet deposition.

4.1.3. Effects of NO_x from aircraft. Emission of additional NO_x from aircraft leads to changes in NO_x concentrations, net chemical ozone production and ozone concentrations as shown in Fig. 5 for the reference case. Due to the relatively short lifetime of NO_x, the increase in NO_x is mainly confined to the flight corridors. The increase in the NO_x concentrations are largest over the eastern part of the North Atlantic Flight Corridor (NAFC), increasing the calculated NO_x concentration by about 50 pptv (35%) in July at 200 hPa. Generally, over the north Atlantic between 45 and 60°N, the increase is about 35%. The calculated increase in NO_x concentrations are higher in the Arctic region than at lower latitudes even if the source of NO_x from aircraft per area is stronger in the tropical/sub-tropical region of the northern hemisphere. This is due to less efficient vertical mixing and longer chemical lifetime of NO_x at higher latitudes.

The increase in net ozone production at 200 hPa during July peaks over the United States, with a maximum extending eastward over the southern parts of the NAFC (Fig. 5, middle panel). The maximum increase in the net production is generally shifted southwards compared to the maximum in the NO_x increase due to dependency of the ozone production on solar radiation, non-linear chemical effects, and probably because more intense convective mixing brings up more reactive hydrocarbons fuelling the ozone production. The combination of these two effects leads to almost twice as high concentrations of hydrogen peroxy radicals (HO_2) over south eastern parts of the United States, than over southern Europe when aircraft emissions of NO_x are included. During January, the increase in the net ozone production at 200 hPa, reach about 0.25 ppbv/day over a broad region (20–50°N, 120°W–70°E).

The calculated increases in net ozone production in other model studies differ significantly. Flatøy and Hov (1996), with a mesoscale CTM, calculates an increase in the diurnal mean net ozone production at the 10.5 km level of 0.7–1.2 ppbv/day over the northern Atlantic and Central Europe during 1–10 July 1991. Dameris

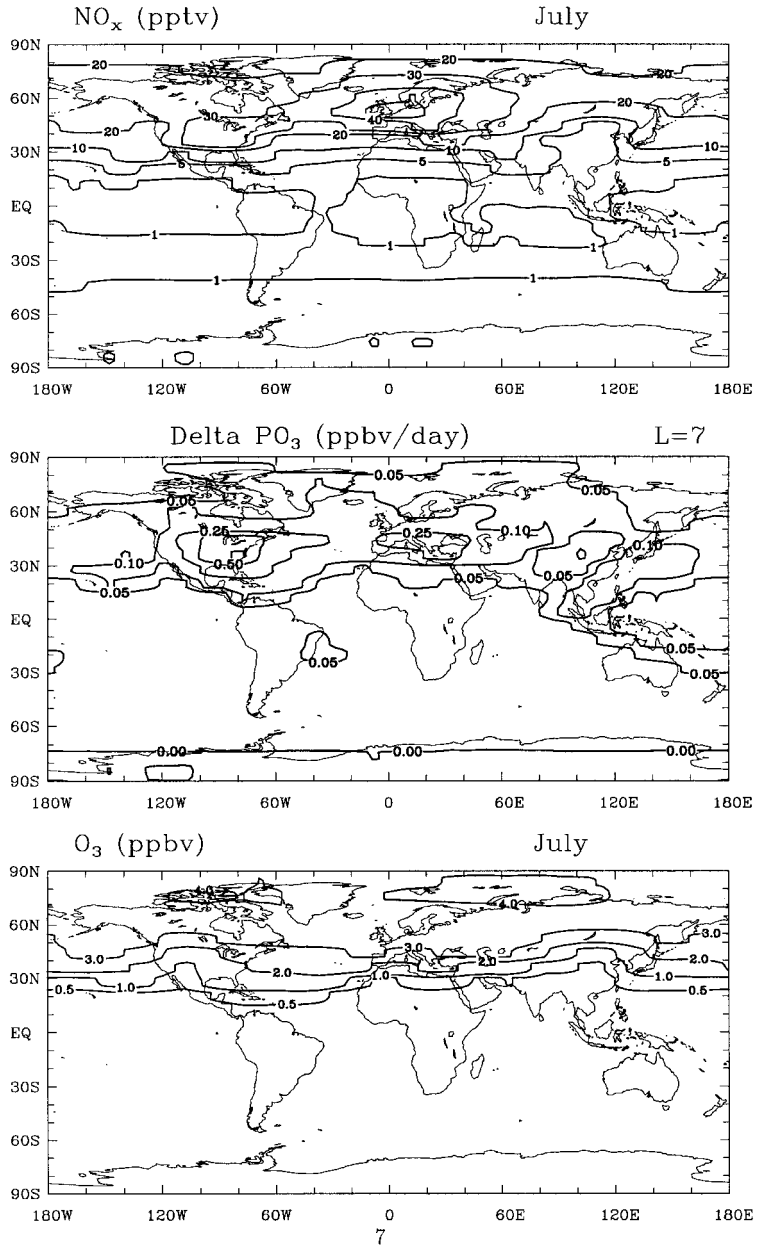

Fig. 5. Calculated increase in NO_x (upper panel, isolines at 1, 5, 10, 20, 30, 40 and 50 pptv), net ozone production (middle panel, isolines at 0.0, 0.1, 0.2, 0.3, 0.4, 0.4, 0.5 and 0.6 ppbv/day), and ozone concentration (lower panel, ppbv) at 200 hPa in the CTM due to NO_x emissions from aircraft in case *R*.

et al. (1998) calculate increases at the 200 hPa level of about 0.12 and 0.08 ppbv/day for January and July respectively with the global 3-D coupled dynamic-chemical model ECHAM3/CHEM. The results obtained in this study (+0.75 ppbv/day over eastern US and +0.35 ppbv/day over Central Europe) are in good agreement with the values obtained by Flatøy and Hov taking into account

the different source strength applied in the two studies (0.85 Tg(N)/yr versus 0.52 Tg(N)/yr in this study). The much lower ozone production efficiency found by Dameris et al. (1998) for July, can be attributed to significantly higher background concentrations of NO_x in July in the ECHAM3/CHEM model (about 300 pptv versus about 150 pptv).

The increase in the ozone concentration is found to be 3–4 ppbv at 200 hPa in July, north of about 45°N (Fig. 5, lower panel). The northward shift in the ozone increase relative to the increase in the ozone production is mainly caused by the longer residence time of ozone in the upper troposphere at higher latitudes. Due to the higher convective activity at lower latitudes, the enhanced ozone concentrations at these latitudes will tend to be mixed downward and be lost by surface deposition.

Brasseur et al. (1998) compare results from this model with results from 3 other global 3-D CTMs, the KNMI model (Wauben et al., 1997), the DLR model (Dameris et al., 1998), and the BISA model (Müller and Brasseur, 1995). All models except the DLR model shows zonally homogeneous ozone increases confined to the region north of 30°N, with a maximum during spring or summer. There are, however, significant differences in the magnitude of the ozone increase between the models. This is mainly attributed to differences in the source strength of the aircraft emissions, non-linear chemistry effects, and to differences in the transport processes in the model. The background NO_x concentrations varies significantly between the models, causing the differences in the ozone production efficiencies. Differences in the transport, in particular the vertical mixing, have a large influence on the amount of ozone produced from aircraft emitted NO_x that remains in the upper troposphere.

4.1.4. Seasonal cycle in the ozone increase. Due to the seasonal cycle in the production and loss rates of ozone, and the seasonal cycle in the transport pattern in the troposphere at mid- and high-latitudes, there is a strong seasonal cycle in the calculated impact of aircraft on upper tropospheric ozone. This is mainly driven by two different factors, which have a completely different seasonal cycle. The convective mixing, which reach a maximum during summer, tends to dilute the ozone maximum by transporting ozone produced aloft downwards where the loss of ozone is more efficient. This favours a winter maximum. On the other hand, the photochemistry leading to ozone production is driven by sunlight, and will in most models give a summer peak in the net ozone production. However, this is complicated by seasonal cycles in the sources of NO_x to the upper troposphere, which can lead to non-linear chemical effects on the ozone production, which overrides the effect of the seasonal cycle of the sunlight (cf. the change in net ozone production by Dameris et al. (1998) discussed above).

This is illustrated in Figs. 6, 7. Fig. 6 shows the zonally averaged increase in ozone due to aircraft emissions for January, May, and July, while Fig. 7 shows the maximum increase in upper tropospheric ozone (integrated between 390 and 150 hPa) occurs in spring and early summer (April–June). The month of May is included in Fig. 6 as the maximum increase in ozone concentrations occurs during this month (6 ppbv, north of 50°N). This is not driven by a corresponding maximum in the increase of the net ozone production, which peaks in July, but rather by slower vertical mixing during spring than summer. The seasonal maximum occurs earlier at lower latitudes (April at 40°N) and tends to propagate northwards into the summer. During winter, the increase in ozone is smaller (about a factor of 2), and is mainly confined to mid-latitudes, due to the lack of sunlight to drive the ozone production at higher latitudes. The more efficient vertical mixing by convection at low latitudes brings the ozone down towards the surface where it is more readily lost by chemical processes and surface deposition (Jacob et al., 1993). This is causing the minimum in the impact on ozone in the tropics. The increase in ozone becomes slightly higher at mid-latitudes in the southern hemisphere, however, the increase is a factor of 10 stronger at northern mid-latitudes, reflecting the large difference in aircraft emissions between the two hemispheres.

4.2. Impacts of lightning and convection

To study how the uncertainties in the lightning source of NO_x and the convective activity affect aircraft induced perturbations, we have performed sensitivity studies with reduced lightning emissions

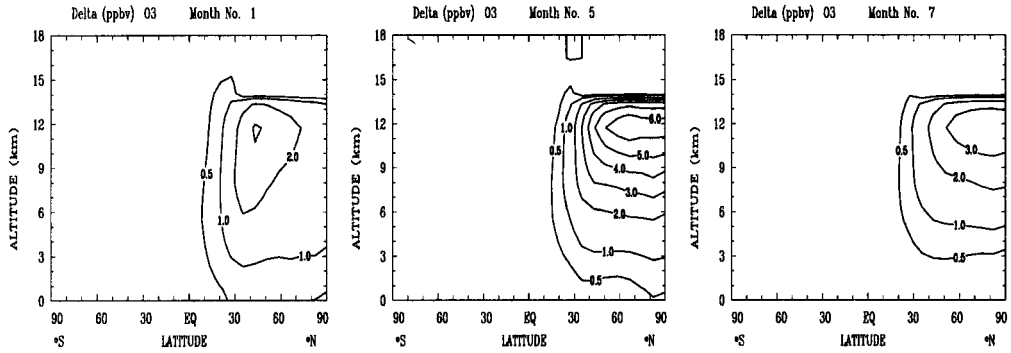

Fig. 6. Calculated increase in zonally averaged ozone concentrations (ppbv) for January, May and July due to emissions of NO_x from aircraft in case *R*.

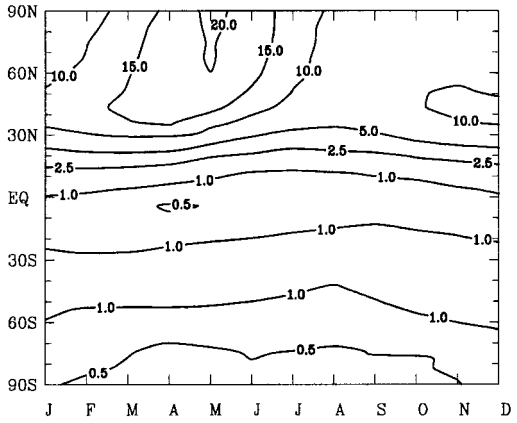

Fig. 7. Calculated zonal averaged change in ozone (kg/km^2) in the upper troposphere (390–150 hPa poleward of 32°, 390–70 hPa at lower latitudes) due NO_x emissions from aircraft for case *R*.

(case LL, 5 Tg(N)/yr), and reduced convective activity (case LC, convective mass fluxes reduced by 67%). As expected reduced emissions of NO_x from lightning (case LL) leads to reduced background concentrations of NO_x, in particular in the upper troposphere (Fig. 8). As a consequence of this, the ozone and OH concentrations also decrease, 3–10% and 5–15%, respectively, in the upper troposphere at 30–60°N in July. In the tropics the influence on ozone is larger (in relative terms) reaching a maximum of about 25% at 4–6 km altitude.

In case LC, the reduced convection reduce the vertical transport of NO_x from below to the upper troposphere. The convective terms of the NO_x budget for case LC_a are about 1/3 of the numbers found for the R_A case (cf. Table 2), so that the net NO_x transport by convection scale with the convective mass flux. Based on this, one would think that the NO_x concentrations in the upper troposphere would be lower in case LC than *R*, but as shown in Fig. 8, the zonal mean concentrations in the CTM actually increase by 10–40% in the upper troposphere at all latitudes. (There is a small local decrease of about 10% over the most polluted regions in Europe and the eastern US.) The ozone concentrations in the upper troposphere are about 15–20% higher at northern midlatitudes (30–80% higher in the tropics), while the OH concentrations decrease slightly (10–20%).

This result is in qualitatively agreement with the results of Lelieveld and Crutzen (1994), but quantitatively the impact appears to be smaller in our model. However, since the contribution from convective transport (updraft and subsidence) is a source of NO_x to the upper troposphere (also in case LC), the mechanism in our model must be different than for the MOGUNTIA model applied by Lelieveld and Crutzen. First, the dynamical lightning source, the vertical distribution of lightning emissions (Subsection 3.2) and the strength of the other NO_x sources in the upper troposphere play a role (Subsection 4.1.2). In addition we find that there are chemical effects linked to the redistribution of nitrogen within the NO_y family in the upper troposphere. Fig. 9 shows the changes of the concentrations of some of the key species due to reduction in the convection. Of particular interest is the shift between HNO_3 and PAN at the 10–12 km level. Table 3 shows the contribution from in situ chemistry and convective transport

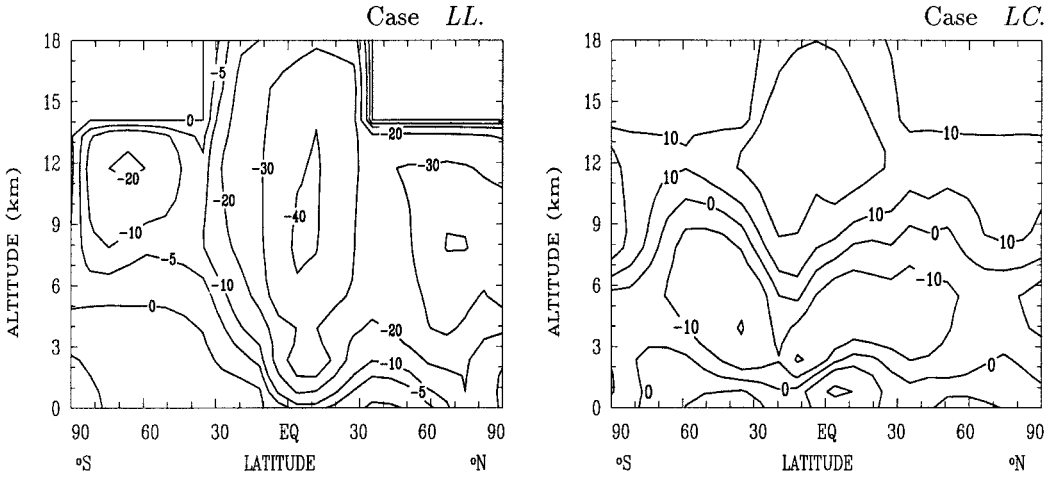

Fig. 8. Calculated change (%) in zonal mean NO_x mixing ratios in July due to reduced lightning emissions (case LL_A versus case R_A) and reduced convective activity (case LC_A versus case R_A, isolines at -25, -10, 0.0, 10 and 25).

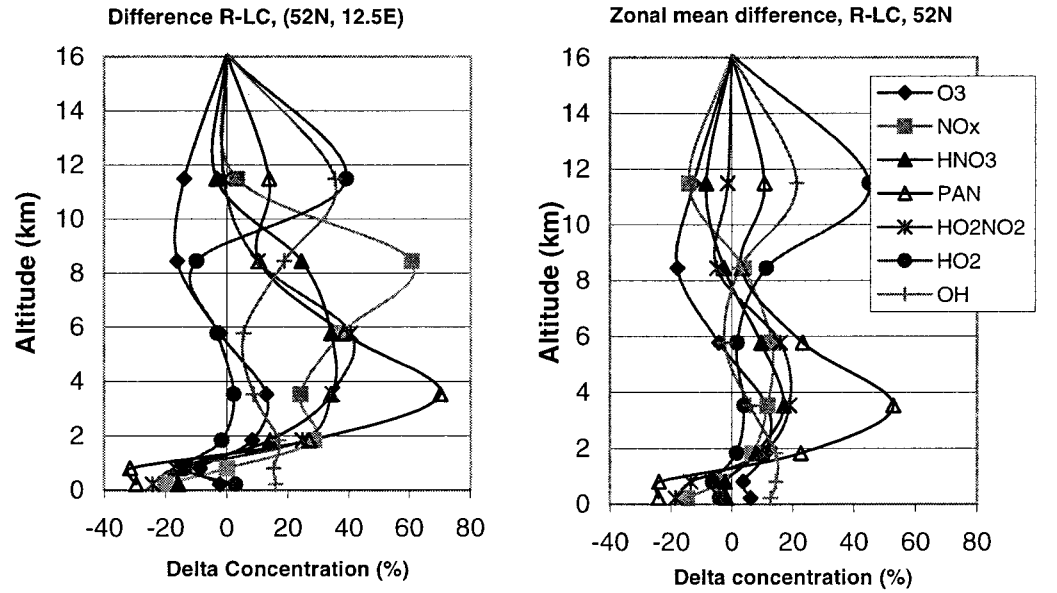

Fig. 9. Calculated change in monthly mean concentration for July (%) of key species as a function of altitude due to reduced convective transport (case R_A versus case LC_A). Left panel: over western Europe. Right panel: zonal average at 52°N.

to the total amount of PAN and HNO_3 in the upper troposphere for July between 32 and 56°N. The convection increases the amount of reactive hydrocarbons and PAN formed in the PBL that reach the upper troposphere. This leads to a significant increase of the amount of NO_x that is transformed to PAN and a small reduction in the formation of HNO_3. Due to the very long lifetime of PAN at the low temperatures in the upper troposphere (photolysis of PAN is ignored in the CTM), the formation of PAN instead of HNO_3 reduce the recycling of NO_x. We believe that this

Table 3. *Sources of PAN and HNO_3 (Gg(N)/month) to the upper troposphere (390–150 hPa) for the latitude band 32–56°N for July for case R_a and LC_a*

	Case R_a	Case LC_a
PAN chemistry	55	28
PAN convection	−8.8	−0.66
HNO_3 chemistry	27	30
HNO_3 convection	7.5	4.2

process, which was not included in the work by Lelieveld and Crutzen (NMHC chemistry not included), is important to understand the apparent discrepancies between the results presented in Table 2 and Fig. 8.

4.2.1. Effects of aircraft emissions in case LL. Input of additional NO_x to the upper troposphere through aircraft activity leads to increased concentrations of NO_x in the upper troposphere (cf. Fig. 5). However, the increase of NO_x is different in case LL and LC, than in case *R* (Figs. 10, 11). In case LL the lower NO_x emissions from lightning leads to less ozone in the upper troposphere than in case *R*. This causes lower OH concentrations and thereby a longer chemical lifetime of NO_x. The perturbation of the NO_x concentrations due aircraft is therefore enhanced in case LL (by up to 1.5 pptv or 5–10% of the total perturbation in case *R*). The increase in net ozone production due to emissions of NO_x from aircraft is generally higher in the LL case than in case *R* (Fig. 10, middle panel), due to the non-linear dependence of the ozone production on the background NO_x levels (Lin et al., 1988; Grooss et al., 1998). Over the East Coast of the USA where the difference is at its maximum (0.2 ppbv/day higher), the monthly mean NO_x concentrations are 40 pptv lower in the LL_A case than in R_A in July. The corresponding enhancement of ozone increase in July due to aircraft emissions (LL versus *R*) is 1.5–2.5 ppbv north of 40°N, with a geographical pattern very similar to the ozone increase in case *R* (Fig. 5, lower panel). South of 20°N, the difference is less than 0.25 ppbv.

4.2.2. Effects of aircraft emissions in case LC. The reduced convective mixing (case LC) leads to a much stronger influence of NO_x from aircraft on the monthly mean upper tropospheric NO_x concentrations during July, compared to case *R* (Fig. 11, upper panel). The increase of NO_x nearly double over the Eastern US and North East Europe due to less downward mixing of the NO_x emitted at altitude. The difference in the change in net ozone production between case LC and *R* is shown in the middle panel of Fig. 11. Even if there is a 30–50% stronger increase in the NO_x perturbation due to emissions from aircraft, the increase in net ozone production is lower in case LC than in case *R*. As for case LL, the difference is most pronounced over the Eastern US, reaching $\div 0.1$ ppbv/day. The difference in the change in the net ozone production is cause by two effects. First, the higher background NO_x levels in case LC (40 pptv higher over the Eastern US in July) leads to less efficient ozone production per additional NO_x molecule emitted from aircraft. Secondly, the reduced convection also suppresses vertical transport of reactive hydrocarbons from the PBL. The amount of HO_2 radicals is 30–40% lower at 200 hPa over the continents in case LC than in case *R*, making the ozone production less efficient.

The resulting change in upper tropospheric ozone is nevertheless higher in case LC than in case *R*, even if less ozone is produced at altitude. The extended lifetime with respect to downward mixing of ozone, means that a larger fraction of the ozone produced by the emissions from aircraft remains in the upper regions of the troposphere. Therefore in July the increase in ozone is enhanced by 1.0–1.5 ppbv north of 40°N and 0.25–0.5 ppbv in the tropics in case LC compared to case *R*.

4.2.3. Seasonal variability. So far we have mainly focused on the results for July. However, there are significant differences in the impacts of lightning and convection over the course of the year. The relative differences (case LL versus *R*, and LC versus *R*) in zonally averaged upper tropospheric ozone change (390–150 hPa) due to emissions of NO_x from aircraft are shown in Fig. 12. Reduced emissions from lightning (LL) lead to a broader spring/summer maximum at mid- and high-latitudes (up to 70% higher increase in ozone at 50°N in August/September). At lower latitudes, where the lightning emissions have their maximum, the differences between case LL and the reference case is less pronounced. This is due to more intense

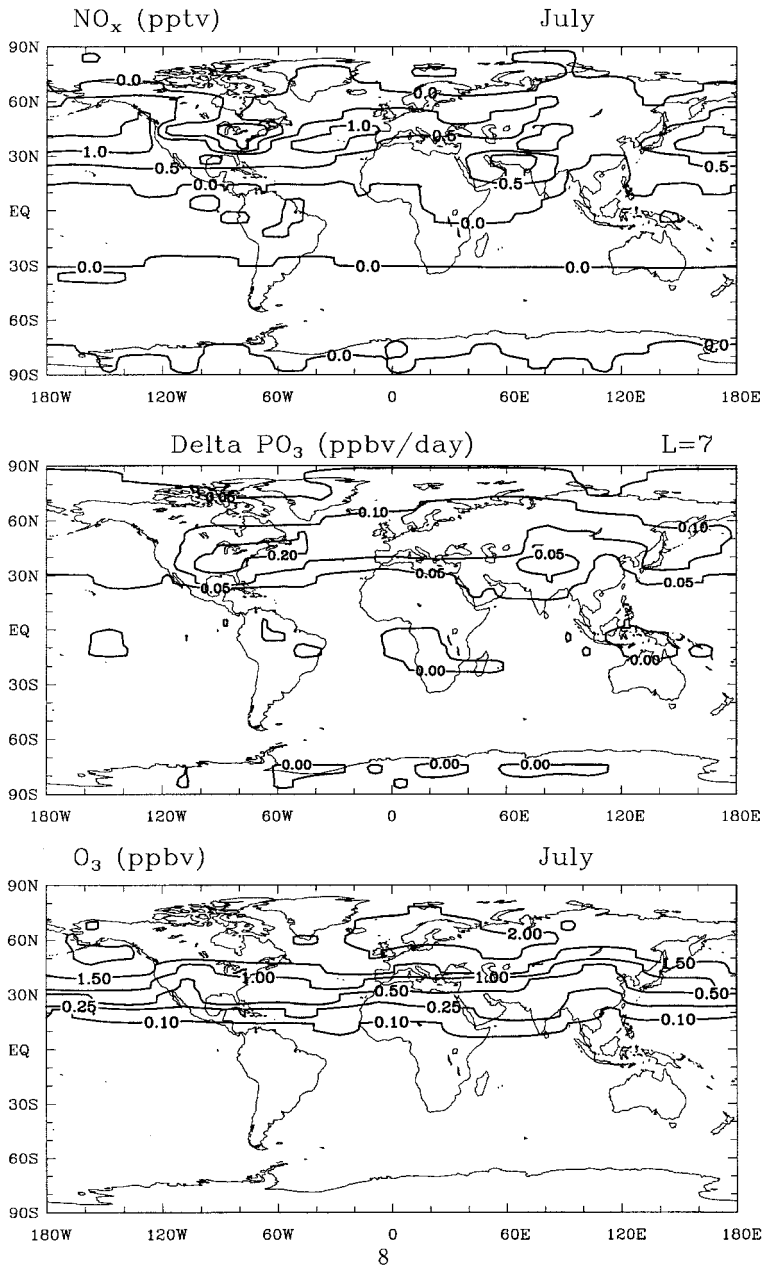

Fig. 10. Calculated difference in the impact of aircraft emissions in case LL versus case *R* at 200 hPa. Upper panel: NO_x (isolines at −0.5, 0.0, 0.5, 1.0, 2.5, 5.0, 7.5, 10.0, and 12.5 pptv). Middle panel: net ozone production (isolines at −0.1, −0.05, 0.0, 0.05, 0.1, and 0.2 ppbv/day). Lower panel: ozone concentration (isolines at 0.0, 0.1, 0.25, 0.5, 1.0, 1.5 and 2.0 ppbv).

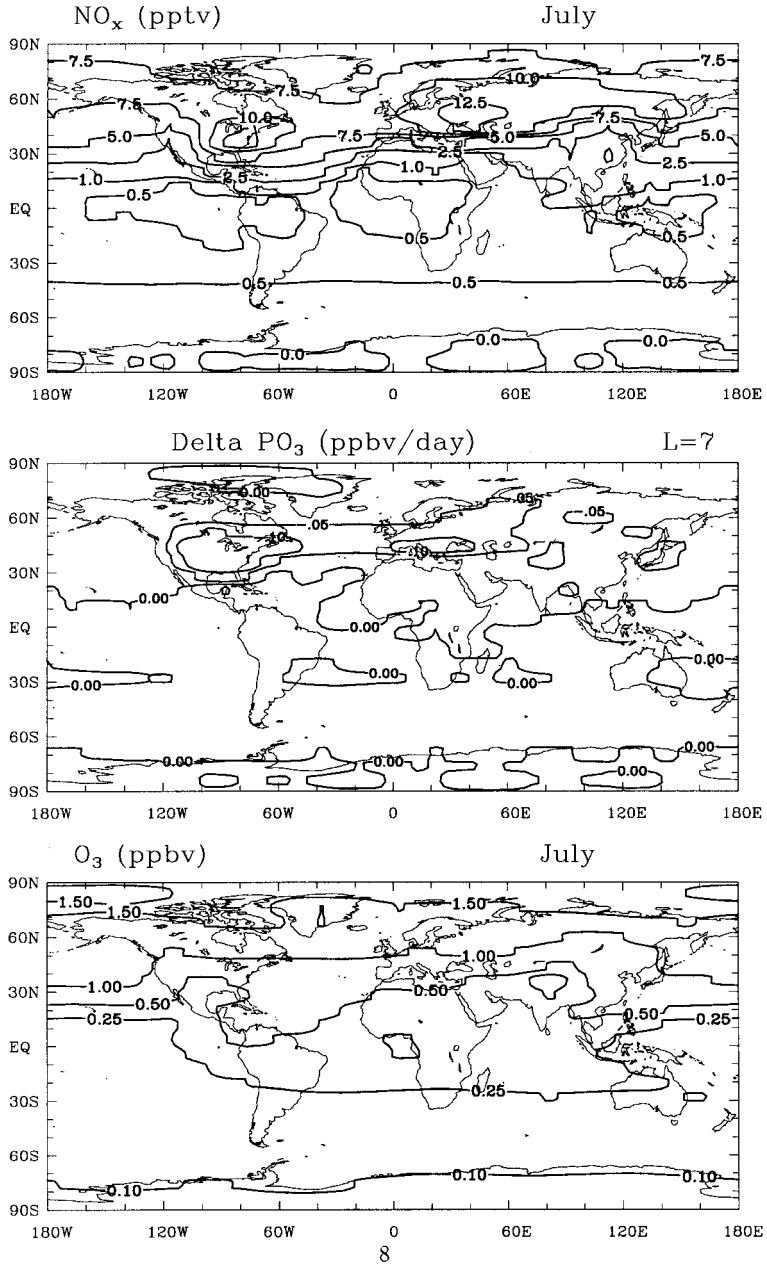

Fig. 11. As for Fig. 10, but for case LC versus case *R*.

convective mixing in these regions, which mix down the increased amount of ozone caused by the emissions from aircraft.

The effect of decreasing the convective mixing (case LC) is also to increase the enhancement of upper tropospheric ozone due to the emissions of NO_x from aircraft at all latitudes and during all seasons. This is due to the prolonged residence time of the ozone produced in the upper troposphere, which more than compensate for the

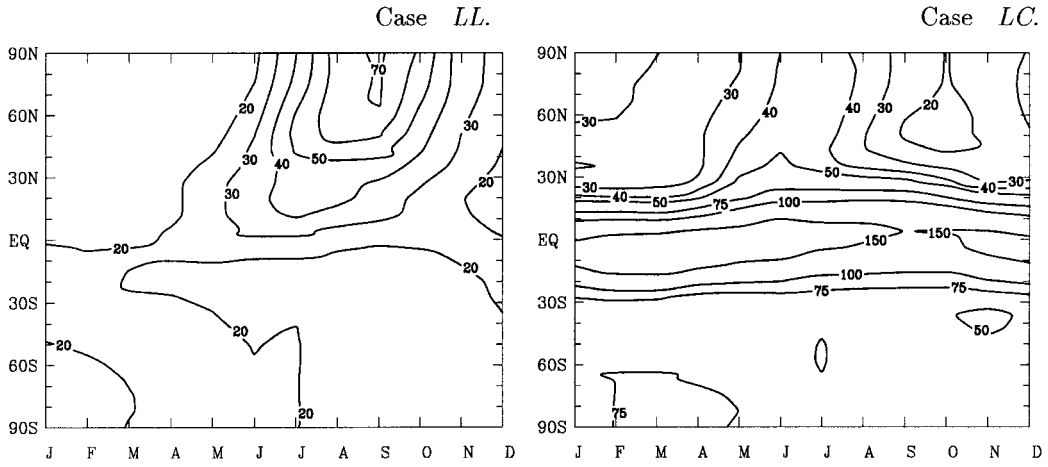

Fig. 12. % difference (versus case *R*) in the integrated change in the mass of ozone in the upper troposphere (390–150 hPa poleward of 32°, 390–70 hPa at lower latitudes) due to emissions from aircraft for cases LL (left) and LC (right).

reduced ozone production efficiency caused by the higher NO_x background levels. The relative effect is particularly strong in the tropics (150% increase). However, the absolute increase in the upper tropospheric ozone column is only about 30% of the increase in the high-latitude region. At northern mid-latitudes the maximum effect occurs during summer, where the increase in ozone is 40–50% higher than in case *R*.

4.2.4. Changes in the upper tropospheric ozone budget. The impact of aircraft emissions is fairly similar for all regions at northern mid-latitudes, but varies significantly between the cases (cf. Figs. 5, 10, 11). The differences between the three cases are due to a combination of non-linear chemical effects and transport effects in the LC case. The emission of NO_x from aircraft leads to increased ozone production, but also to increased loss from the upper troposphere by transport processes due to steeper vertical gradients in the ozone profile. Also the chemical loss, which is largely proportional to the ozone concentration, is enhanced due to the increase in the ozone concentrations. As shown in Fig. 13 all the terms in the ozone budget can change significantly when aircraft emissions of NO_x are included. In all cases there is an increase in the photochemical ozone production, which is not balanced by an increase in the chemical loss. This leads to an increased vertical gradient between the lower troposphere and the regions directly affected by the aircraft emissions. Thus, the loss due to vertical mixing will increase which is reflected in the convection and vertical advection terms. The approximately equal effect for each region for each case is due to the fast zonal mixing which smooth the differences in ozone production and loss processes between the regions.

A somewhat surprising finding was that the increase in the net chemical ozone production was smallest in case LC, in particular over the continental regions of North America and Asia. However, as discussed above, the background NO_x levels increase in case LC compared to case *R*, which reduce the ozone production efficiency. Compared to case LL, the higher emissions from lightning give higher background NO_x levels and therefore the ozone production becomes less efficient. Nevertheless, the increase in ozone concentrations due to emissions of NO_x from aircraft, is found to be highest in case LC, because the reduced loss of ozone from the upper troposphere by downward mixing more than compensates for the lower production.

4.2.5. Ozone production efficiency. A key question is whether there are pronounced differences between the regions with respect to the ozone production efficiency of aircraft emitted NO_x, and

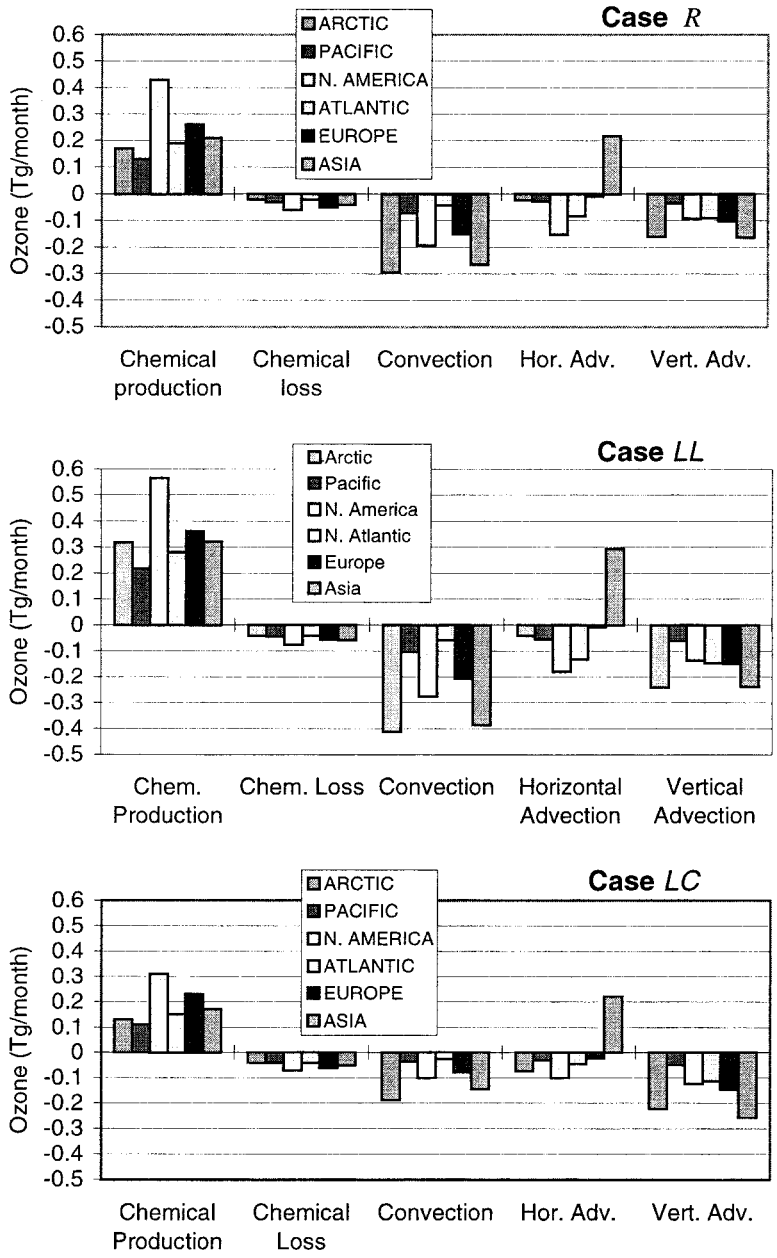

Fig. 13. Changes in monthly mean (July) budget terms for ozone in the upper troposphere (390–150 hPa) due to inclusion of NO_x emissions from aircraft in case *R*, with lower lightning emissions (LL), and lower convection (LC) cases, respectively.

whether the production efficiency depends strongly on the assumptions about lightning and convection activity. This question also relates to how changes in future aircraft emissions, which are likely to cause in increase at lower latitudes, in particular over Asia, will affect the distribution of upper tropospheric ozone.

To address this issue, we have calculated an

ozone production efficiency (α) given as (for case R):

$$\alpha_R = \Delta PO_3(R)/\Delta EM_{NO_x},$$

where ΔPO_3 and ΔEM_{NO_x} are the increases in chemical ozone production and emissions of NO_x from aircraft within a given region of the atmosphere. Values for α have been calculated for each experiment (α_R, α_{LL}, and α_{LC}) and for each region (Table 4). The α values could be somewhat influenced by transport of aircraft emitted NO_x from one region to another, which then will cause ozone production downstream, thereby enhancing the calculated α values in that region. However, the calculated increase in NO_x and net ozone production shown in Fig. 5 indicates that most of the NO_x from aircraft is processed in the region where it is emitted. This definition of α instead of what maybe seem more natural as the ratio between the change in total ozone mass and the NO_x emissions, is a lot cheaper with respect to computing time. The latter definition would require separate model calculations with and without aircraft for each region. Given the rapid zonal mixing of ozone in the upper troposphere, evident from the homogeneous signal in ozone (Figs. 5, 10, 11), the definition applied in this work is useful to be able to compare the efficiency of the chemistry in different regions.

To study the impact of lightning and convection ozone production enhancements factors

$$\beta_{LL} = (\alpha_{LL} - \alpha_R)/\alpha_R,$$

and

$$\beta_{LC} = (\alpha_{LC} - \alpha_R)/\alpha_R,$$

were also calculated for each region. Higher absolute values of β indicate that the region is specifically sensitive to the assumptions made about the lightning source or the convective activity.

As expected the ozone production efficiency is smallest for the continental regions due to the higher background of NO_x caused by upward transport of PBL air by deep convection, and higher emissions of NO_x from lightning. The highest α-value is found over the Pacific, where background NO_x levels are very low (cf. Fig. 3). When the lightning source of NO_x is reduced to 5 Tg(N)/yr in case LL, the ozone production efficiency increases in all regions as expected. However, it is somewhat surprising that enhancement of the ozone production efficiency (the β factor) is higher for the marine regions and for the Arctic where the lightning emissions are lower. This can be explained by the coupling of deep convection and lightning emissions in the model, and by the non-linearity of the ozone chemistry. Over the most polluted continental regions (North America and Europe) the elevated NO_x levels due to convection means that the relative contribution to the upper tropospheric NO_x levels by lightning is smaller. The enhancement of the ozone production efficiency of the NO_x emitted from aircraft is therefore smaller in these regions.

The value of β_{LC} is always negative because of the smaller increase in net chemical ozone production in this case, as discussed above. The tropical region appears to be the most sensitive region as convection is more important for upper tropospheric NO_x concentrations in the tropics than in the other regions (cf. Fig. 8).

Table 4. *Ozone production efficiency, α (kg O_3/kg NO_x(N)), and efficiency enhancements, β, in the upper troposphere (390–150 hPa) for the month of July*

Region	α_R	α_{LL}	α_{LC}	β_{LL}	β_{LC}
Arctic	77.3	144	59.1	0.86	−0.24
Pacific	119	200	101	0.68	−0.15
N. America	49.7	65.4	35.8	0.32	−0.28
N. Atlantic	86.7	128	68.5	0.47	−0.21
Europe	30.1	41.8	26.7	0.39	−0.12
Asia	22.9	34.9	18.6	0.52	−0.19
NH tropics	86.5	112.5	67.3	0.30	−0.41

5. Conclusions

A global 3-D CTM has been applied to study the impact of uncertainties in lightning emissions of NO_x and deep convective activity on the changes in tropospheric ozone due to NO_x emissions from aircraft. A case with reduced emissions of NO_x from lightning (5 Tg(N)/yr, case LL) and a case with reduced convective activity (number of events reduced by 67%, case LC) have been compared with the reference case (12 Tg(N)/yr from lightning, case R). In the reference case we find a zonally homogeneous increase in upper tropospheric ozone concentrations in July of

3–4 ppbv north of 40°N at 200 hPa altitude. However, the maximum increase is found somewhat earlier (April–May), reaching 5–6 ppbv.

In both the perturbation cases (LL and LC) we find enhanced impact of NO_x from aircraft on ozone. The main mechanism in case LL is to lower the background levels of NO_x in the upper troposphere, thereby increasing the ozone production efficiency per NO_x molecule emitted from aircraft. The maximum enhancement (50–70%) in the ozone increase due to NO_x from aircraft, compared to the reference case, is found at mid- and high-latitudes during summer and early fall.

In case LC the background concentrations of NO_x increases by 10–40%. This is found to be mainly a chemical effect through redistribution of species within the NO_y family. Reduced formation of PAN and increased formation of nitric acid enhance the recycling of NO_x in the upper troposphere in case LC. The ozone production efficiency of NO_x emitted from aircraft is therefore less than in case *R* and LL. However, the reduced loss of ozone through transport compensates for this, giving the enhancement of ozone from aircraft in this case.

Uncertainty in the convective activity is found to cause the largest uncertainty in the increase of ozone in the upper troposphere (390–150 hPa), in particular in the tropical region. In the region of maximum ozone perturbations (40°N, spring/summer) both lightning and convection are found to cause about 40% uncertainty in the predicted change of ozone. Assuming that the growth in air-traffic will be most pronounced at lower latitudes (Brasseur et al., 1998), and the higher climate sensitivity at low latitudes, makes further studies related to convective mixing important in future aircraft research. However it should be kept in mind that other factors not discussed in this paper (unknown chemistry leading to HNO_3 to NO_x conversion), vertical distribution of lightning the source, and impacts of growth in surface emissions of NO_x, could be of equal importance.

The impact on upper tropospheric ozone due to aircraft emissions of NO_x was found to be very sensitive to the convective activity in the low latitude regions (cf. Figs. 6, 8). In light of the higher climate sensitivity of ozone perturbations at low latitudes this can add up to a significant uncertainty in the global radiative forcing due to aircraft emissions. As shown in Berntsen et al. (1997), the radiative forcing at low latitudes can be as much as a factor of 3 more sensitive to tropospheric ozone changes due to higher surface temperatures, stronger vertical temperature gradients, and less clouds at low latitudes. In addition, estimates of future trends in emissions from aircraft predict a higher growth rate at low latitudes than at mid- and high-latitudes (Vedontham and Oppenheimer, 1994). It is therefore important to be particularly aware of the tropical regions when assessing the climate impact of ozone increases due emissions from aircraft.

6. Acknowledgements

This work is been supported by the European Community grant (AEROCHEM, Contract No. ENV4-CT95-0144). We would like to thank C. Price for providing the lightning emission data. This work has also received support from The Research Council of Norway through a grant of computing time.

7. Appendix

NO_x from lightning

This Appendix describes how the 2-dimensional (latitude versus longitude) NO_x emission numbers from lightning given by Price et al. (1997a) have been distributed in space and time for use in the CTM. The procedure links the emissions to the actual (8-h) convective activity in the meteorological input data, giving a so-called dynamical lightning source.

The input data to the CTM (cf. Section 2) includes the number of deep convective events every 8th hour (N_{dc}), and cloud top height of deep convective clouds (H, in km), averaged over 120 h. Based on the parameterisation of the number of flashes for continental and marine clouds as a function of cloud top height given in Price et al. (1997a), the number of flashes for each gridcell in the CTM for each 8-h period (F_c and F_m for continental and marine gridcells respectively) was calculated by:

$$F_c(\theta, \phi, t) = N_{dc} \times 3.44 \times 10^{-5} H^{4.92},$$

$$F_m(\theta, \phi, t) = N_{dc} \times 6.40 \times 10^{-4} H^{1.73},$$

where θ is longitude, ϕ is latitude, and t is time.

Similarly, the total number of flashes for continental (FT_c) and marine (FT_m) regions respectively for each latitude band in the CTM and each month were calculated by

$$FT_c(\phi, m) = \sum_{0,t} F_c(\theta, \phi, t),$$

$$FT_m(\phi, m) = \sum_{0,t} F_m(\theta, \phi, t),$$

where the sum is over all 8-h periods (t) during a month (m) and all longitudes (θ), for continental and marine grid-cells respectively.

From the emission data from Price et al. (1997a), zonally averaged emissions for continental (grid cells with land-fractions greater than 0.25) and marine regions respectively were calculated ($ZPL_c(\phi, m)/ZPL_m(\phi, m)$). The source strength of NO_x from lightning during each 8-h period in each grid column in the CTM was then calculated by

$$PL(\theta, \phi, t) = ZPL_c(\theta, m) \times F_c(\theta, \phi, t)/FT_c(\phi, m)$$

for continental grid-cells, and by

$$PL(\theta, \phi, t) = ZPL_m(\phi, m) \times F_m(\theta, \phi, t)/FT_m(\phi, m)$$

for marine grid-cells.

The vertical distribution of the NO_x from lightning is discussed in Subsection 3.2.2.

REFERENCES

Arnold, F., Klemm, M., Schneider, J., Bürger, V., Droste-Franke, B., Kirchner, G., Preissler, B., Jung, A. and Dann, W. 1997a. Trace gas measurements by aircraft based ion molecule mass spectrometry. In: *Pollution from aircraft emissions in the North Atlantic Flight Corridor (POLINAT)* (ed. Schumann, U.). Report EUR 16978 EN, 303 pp. Brussels, Belgium.

Berntsen, T. and Isaksen, I. S. A. 1997. A global 3-D chemical transport model for the troposphere (1) Model description and CO and ozone results. *J. Geophys. Res.* **102**, 21,239–21,280.

Berntsen, T. Isaksen, I. S. A., Fuglestvedt, J. S., Alsvik Larsen, T., Stordal, F., Freckleton, R. S. and Shine, K. P. 1997. Effects of anthropogenic emissions on tropospheric ozone and its radiative forcing. *J. Geophys. Res.* **102**, 28,101–28,281.

Brasseur, G. P., Müller, J.-F. and Granier, C. 1996. Atmospheric impact of NO_x emissions by subsonic aircraft: a three-dimensional model study. *J. Geophys. Res.* **101**, 1423–1428.

Brasseur, G. P., Cox, R. A., Hauglustaine, D., Isaksen, I. S. A., Lelieveld, J., Lister, D. H., Sausen, R., Shumann, U., Wahner, A. and Wiesen, P. 1998. European scientific assessment of the atmospheric effects of aircraft emissions. *Atmos. Environment* **32**, 2329–2418.

Chatfield, R. B. 1994. Anomalous HNO_3/NO_x ratio of remote tropospheric air — conversion of HNO_3 to formic acid and NO_x. *Geophys. Res. Lett.* **21**, 2705–2708.

Crutzen, P. J. 1973. A discussion of the chemistry of some minor constituents in the stratosphere and troposphere. *Pure Appl. Geophys.* **106–108**, 1385–1399.

Dentener, F. and Crutzen, P. J. 1993. Reaction of N_2O_5 on tropospheric aerosols: Impact on the global distributions of NO_x, O_3 and OH. *J. Geophys. Res.* **98**, 7149–7163.

Dameris, M., Grewe, V., Köhler, I, Sausen, R., Bruhl, C., Gross, J.-U. and Steil. B. 1998. Impact of aircraft NO_x emissions on tropospheric and stratospheric ozone. Part II: 3-D model results. *Atmosheric Env.* **32**, 3185–3199.

Emmons, L. K. et al. 1997. Climatologies of NO_x and NO_y. A comparison of data and models. *Atmos. Environ.* **31**, 1851–1904.

Flatøy, F. and Hov, Ø. 1996. Three-dimensional model studies of the effect of NO_x emissions from aircraft on ozone in the upper troposphere over Europe and the North Atlantic. *J. Geophys. Res.* **101**, 1401–1422.

Flatøy, F. and Hov, Ø. 1997. NO_x from lightning and the calculated chemical composition of the free troposphere. *J. Geophys. Res.* **102**, 21,373–21,382.

Forster, P. M. de F., Johnson, C. E., Law, K. S., Pyle, J. A. and Shine, K. P. 1996. Further estimates of radiative forcing due to tropospheric ozone changes. *Geophys. Res. Lett.* **23**, 3321–3324.

Franzbleau, E. and Popp, C. J. 1989. Nitrogen oxides produced by lightning. *J. Geophys. Res.* **94**, 11,089–11,104.

Fuglestvedt, J. S., Isaksen, I. S. A. and Wang, W.-C. 1996. Estimates of indirect global warming potentials for CH_4, CO and NO_x, *Clim. Change* **34**, 405–437.

Gallardo, L. and Cooray, V. 1996. Could cloud-to-cloud discharges be as effective as cloud-to-ground discharges in producing NO_x. *Tellus* **48B**, 641–651.

Goldenbaum, G. C. and Dickerson, R. R. 1993. Nitric oxide production by lightning discharges. *J. Geophys. Res.* **98**, 18,333–18,338.

Grooss, J.-U., Brühl, C. and Peter, T. 1998. Impact of aircraft emissions on tropospheric and stratospheric ozone. Part I: Chemistry and 2-D model results. *Atmospheric Env.* **32**, 3173–3184.

Hansen, J., Russel, G., Rind, D., Stone, P., Lacis, A., Lebedeff, S., Ruedy, R. and Travis, L. 1983. Efficient three dimensional global models for climate studies: Models I and II. *Mon. Weather Rev.* **111**, 609–662.

Hauglustaine, D. A., Granier, C., Brasseur, G. P. and Megie, G. 1994. The importance of atmospheric chem-

istry in the calculation of radiative forcing on the climate system. *J. Geophys. Res.* **99**, 1173–1186.

Hauglustaine, D. A., Ridley, B. A., Solomon, S., Hess, P. G. and Madronich, S. 1996. HNO_3/NO_x ratio in the remote troposphere during MLOPEX 2: Evidence for nitric acid reduction on carbonaceous aerosols? *Geophys. Res. Lett.* **23**, 2609–2612.

Hesstvedt, E., Hov, Ø. and Isaksen, I. S. A. 1978. Quasi steady-state approximation in air pollution modeling: Comparison of two numerical schemes for oxidant prediction. *Int. J. Chem. Kinet.* **X**, 971–994.

Intergovernmental Panel on Climate Change (IPCC). 1992. *Climate change 1992: the supplementary report to the IPCC scientific assessment* (eds. Houghton, J. T., Callander, B. A. and Varney, S. K.), 200 pp. Cambridge Univ. Press, New York.

Intergovernmental Panel on Climate Change (IPCC). 1995. *Climate change 1995: the science of climate change* (eds. Houghton, J. T. et al.), 572 pp. Cambridge Univ. Press, New York.

Intergovernmental Panel on Climate Change (IPCC). 1999. *Special teport on aviation and the global atmosphere*, in press.

Isaksen, I. S. A., Hov, Ø. and Hesstvedt, E. 1978. Ozone generation over rural areas. *Environ. Sci. Technol.* **12**, 1279–1284.

Jacob, D. J., Logan, J. A., Gardener, G. M., Yevich, R. M., Spivakovsky, C. M., Wofsy, S. C., Sillman, S. and Prather, M. J. 1993. Factors regulating ozone over the United States and its export to the global atmosphere. *J. Geophys. Res.* **98**, 14,817–14,826.

Jacob, D. J., Heikes, B. J., Fan, S.-M., Logan, J. A., Mauzerall, D. L., Bradshaw, J. D., Singh, H. B., Gregory, G. L., Talbot, R. W., Blake, D. R. and Sache, G. W. 1996. Origin of ozone and NO_x in the tropical troposphere: A photochemical analysis of aircraft observations over the South Atlantic basin. *J. Geophys. Res.* **101**, 24,235–24,250.

Jacob, D. J., Prather, M. J., Rasch, P. J., Shia, R.-L., Balkanski, Y. J., Beagley, S. R., Bergmann, D., Blackshear, W. T., Brown, M., Chiba, M., Chipperfield, M. P., de Grandpré, K., Dignon, J. E., Feichter, J., Genthon, C., Grose, W. L., Kasibathla, P. S., Köhler, I., Kritz, M. A., Law, K., Penner, J. E., Ramonet, M., Reeves, C. E., Rotman, D. A., Stockwell, D. Z., Van Velthoven, P. F. J., Verver, G., Wild, O., Yang, H. and Zimmermann, P. 1997. Evaluation and intercomparison of global atmospheric models using ^{222}Rn and other short lived species. *J. Geophys. Res.* **102**, 5953–5970.

Jaffe, D., Berntsen, T. K. and Isaksen, I. S. A. 1997. A global three-dimensional chemical transport model for the troposphere (2) Nitrogen oxides and non-methane hydrocarbon results. *J. Geophys. Res.* **102**, 21,281–21,296.

Jenkins, G. 1996. *Aviation fuel business, world-wide*. Sunningdale Publ. UK, ISBN 1 872546 11 0.

Kylling, A., Stamnes, K. and Tsay, S.-C. 1995. A reliable and efficient two-stream algorithm for spherical radiative transfer: documentation of accuracy in realistic layered media. *J. Atmos. Chem.* **21**, 115–150.

Köhler, I., Sausen, R. and Reinberger, R. 1997. Contribution of aircraft emissions to the atmospheric NO_x content. *Atmospheric Env.* **31**, 1801–1818.

Lacis, A. A., Wuebbles, D. J. and Logan, J. A. 1990. Radiative forcing of climate by changes in the vertical distribution of ozone. *J. Geophys. Res.* **95**, 9971–9981.

Lee, D. S., Köhler, I., Grobler, E., Rohrer, F., Sausen, R., Gallardo-Klenner, L., Olivier, J. G. J., Dentener, F. J. and Bouwman, A. F. 1997. Estimations of global NOx emissions and their uncertainties. *Atmospheric Env.* **31**, 1735–1749.

Lelieveld, J. and Crutzen, P. J. 1994. Rôle of deep convection in the ozone budget of the troposphere. *Science* **264**, 1759–1761.

Lelieveld, J. and van Dorland, R. 1995. Ozone chemistry changes in the troposphere and consequent radiative forcing of climate. In: *Atmospheric ozone as a climate gas*. NATO ASI Ser. I, vol. 32 (eds. Wang, W.-C. and Isaksen, I. S. A.), pp. 227–258. Springer-Verlag, New York.

Levine, J. S., Rogowski, R., Gregory, G. L., Howell, W. E. and Fishman, J. 1981. Simultaneous measurements of NO_x, NO and O_3 production in laboratory discharge: Atmospheric implications. *Geophys. Res. Lett.* **8**, 357–360.

Lin, X., Trainer, M. and Liu, S. C. 1988. On the nonlinearity of the tropospheric ozone production. *J. Geophys. Res.* **93**, 15,879–15,888.

McKeen, S. A., Gierczak, T., Burkholder, J. B., Wennberg, P. P., Hanisco, T. F., Keim, E. R., Gao, R.-S., Liu, S.-C., Ravishankara, A. R. and Fahey, D. W. 1997. The photochemistry of acetone in the upper troposphere: a source of odd-hydrogen radicals. *Geophys. Res. Lett.* **24**, 3177–3180.

Müller, J.-F. 1992. Geographical distribution and seasonal variation of surface emissions and deposition velocities of atmospheric trace gases. *J. Geophys. Res.* **97**, 3787–3804.

Müller, J.-F. and Brasseur, G. 1995. IMAGES: A three-dimensional chemical transport model of the global troposphere. *J. Geophys. Res.* **100**, 16,445–16,490.

Nüsser, H. G. and Scmitt, A. 1996. *Sclussberict zum forschungsvorhaben Berechung der Emissionsverteilung und deren trends*. BMBF-Förderzeichen: 01 LL 9212/7, 108 pp.

Prather, M. 1986. Numerical advection by conservation of second-order moments. *J. Geophys. Res.* **91**, 6671–6681.

Prather, M., McElroy, M., Wofsy, S., Russel, G. and Rind, D. 1987. Chemistry of the global troposphere: fluorocarbons as tracers of air motion. *J. Geophys. Res.* **92**, 6579–6613.

Price, C. and Rind, D. 1993. What determines the cloud-to-ground fraction in thunderstorms. *Geophys. Res. Lett.* **20**, 463–466.

Price, C., Penner, J. and Prather, M. 1997a. NO_x from

lightning (1). Global distribution based on lightning physics. *J. Geophys. Res.* **102**, 5929–5941.

Price, C., Penner, J. and Prather, M. 1997b. NO_x from lightning (2). Constraints from the global atmospheric circuit. *J. Geophys. Res.* **102**, 5943–5951.

Roelofs, G. J. and Lelieveld, J. 1995. Distribution and budget of O_3 in the troposphere calculated with a chemistry general circulation model. *J. Geophys. Res.* **100**, 20,983–20,998.

Rossow, W. B. and Schiffer, R. A. 1991. ISCCP cloud data products. *Bull. Am. Meteorol. Soc.* **72**, 2–20.

Schlager, H., Schulte, P., Ziereis, H., Konopka, P., Schumann, U., Fheigl, Ch., Marquardt, R. and Huntreiser, H. 1997. Aircraft-borne measurements of NO_x, O_3 and CO_2. In: *Pollution from aircraft emissions in the North Atlantic flight corridor (POLINAT)* (ed. Schumann, U.). Report EUR 16978 EN, 303 pp. Brussels, Belgium.

Schumann, U. (ed). 1997a. *Pollution from aircraft emissions in the North Atlantic flight corridor (POLINAT)*. Report EUR 16978 EN, 303 pp. Brussels, Belgium.

Schumann, U. 1997b. The impact of nitrogen oxide emissions from aircraft upon the atmosphere at flight altitudes — results from the AERONOX project. *Atmospheric. Env.* **31**, 1723–1734.

Singh, H. B., Kanakidou, M., Crutzen, P. J. and Jacob, D. J. 1995. High concentrations and photochemical fate of oxygenated hydrocarbons in the global troposphere. *Nature* **378**, 50–54.

Singh, H. B. et al. 1996a. Reactive nitrogen and ozone over the western Pacific: Distribution, partitioning, and sources. *J. Geophys. Res.* **101**, 1793–1808.

Singh, H. B. et al. 1996b. Impact of biomass burning emissions on the composition of the South Atlantic troposphere: Reactive nitrogen and ozone. *J. Geophys. Res.* **101**, 24,203–24,219.

Strand, A. and Hov, Ø. 1996. The impact of man-made and natural NO_x emissions on upper tropospheric ozone: A two-dimensional model study. *Atmospheric. Env.* **30**, 1291–1303.

Stevenson, D. S., Collins, W. J., Johnson, C. E. and Derwent, R. G. 1997. The impact of aircraft nitrogen oxide emissions on the tropospheric ozone studied with a 3D Lagrangian model including fully diurnal chemistry. *Atmospheric Env.* **31**, 1837–1850.

Vedontham, A. and Oppenheimer, M. 1994. *Aircraft emissions and the global atmosphere; long-term scenarios*. Environmental Defence Found, New York.

Wang, W.-C. and Sze, N. D. 1980. Coupled effects of atmospheric N_2O and O_3 on the Earth's climate. *Nature* **286**, 589–590.

Wauben, W. M. F., van Velthoven, P. F. J. and Kelder, H. 1997. A 3D chemistry transport model study of changes in atmospheric ozone due to aircraft NO_x emissions. *Atmospheric. Env.* **31**, 1819–1836.

WMO, 1995. Scientific assessment of ozone depletion. Global ozone research and monitoring project. Rep. 37, Geneva.